Journal of Magnetic Resonance **145,** 161–172 (2000)
doi:10.1006/jmre.2000.2085, available online at http://www.idealibrary.com on IDEAL®

Relaxation-Induced Dipolar Exchange with Recoupling—An MAS NMR Method for Determining Heteronuclear Distances without Irradiating the Second Spin

Kay Saalwächter*,† and Klaus Schmidt-Rohr*,[1]

*Department of Polymer Science and Engineering, University of Massachusetts, Amherst, Massachusetts 01003; and †Max-Planck-Institute for Polymer Research, Postfach 3148, D-55021 Mainz, Germany

Received November 15, 1999; revised March 6, 2000

A new magic-angle spinning NMR method for distance determination between unlike spins, where one of the two spins in question is *not* irradiated at all, is introduced. Relaxation-induced dipolar exchange with recoupling (RIDER) experiments can be performed with conventional double-resonance equipment and utilize the familiar π-pulse trains to recouple the heteronuclear dipolar interaction under magic-angle spinning conditions. Longitudinal relaxation of the passive spin during a delay between two recoupling periods results in a dephasing of the heteronuclear coherence and consequently a dephasing of the magnetization detected after the second recoupling period. The information about the dipolar coupling is obtained by recording normalized dephasing curves in a fashion similar to the REDOR experiment. At intermediate mixing times, the dephasing curves also depend on the relaxation properties of the passive spin, i.e., on single- and double-quantum longitudinal relaxation times for the case of $I = 1$ nuclei, and these relaxation times can be estimated with this new method. To a good approximation, the experiment does not depend on possible quadrupolar interactions of the passive spin, which makes RIDER an attractive method when distances to quadrupolar nuclei are to be determined. The new method is demonstrated experimentally with ^{14}N and ^{2}H as heteronuclei and observation of ^{13}C in natural abundance.

Key Words: **REDOR; relaxation; distance measurements; recoupling; dipolar couplings; CODEX; DEAR.**

INTRODUCTION

Magic-angle spinning (MAS) NMR methods for the determination of heteronuclear dipolar couplings in solids are of great interest for the investigation of structure and dynamics in solids, particularly in amorphous materials, where scattering methods cannot be applied. The application of π-pulse trains with spacings of half rotor periods to recouple the heteronuclear dipolar interaction in highly resolved MAS spectra has proven to be a universally applicable scheme for the determination of ^{13}C-heterospin dipolar coupling constants. Starting from the initial REDOR (rotational-echo double-resonance) method (*1*), several extensions of this idea have been presented, such as its use in two-dimensional heteronuclear dipolar correlation experiments for the investigation of torsion angles in peptides (*2*) and proteins (*3*), site-resolved dynamics in more complex materials (*4, 5*), or two-dimensional separation of ^{2}H quadrupolar powder spectra by ^{13}C isotropic chemical shifts (*6*). Also, modifications have been devised to extend the applicability of REDOR to quadrupolar systems, where large quadrupolar couplings interfere with a perfect inversion of the spins by a π-pulse of finite length. As remedies for the excitation problems of quadrupolar spins, composite pulses (*7*) or adiabatic passage pulses (REAPDOR, rotational-echo, adiabatic-passage, double-resonance (*8*)) have been proposed.

A limitation of the aforementioned methods is that the theoretical analysis of composite-pulse REDOR and REAPDOR data is somewhat involved, since the amount of dipolar dephasing is dependent on the quadrupolar coupling constants, which in turn complicate the spin dynamics under the pulses. Thus, an extremely careful spectrometer setup and calibration are essential. We present here a new MAS method for determining weak dipolar coupling constants between naturally abundant ^{13}C and quadrupolar nuclei (in fact, the method also works for pairs of spin-$\frac{1}{2}$ heteronuclei) *without irradiating* the heterospin in question. Thus, only a double-resonance probe is needed, and no additional hardware for the irradiation of the additional spins is required.

The method uses the familiar π-pulse train to recouple the heteronuclear dipolar interaction, which is essentially removed by MAS. Exchange occurs due to the effects of T_1 relaxation on the anti-phase coherences associated with the heteronucleus. This effect was observed by Frydman and co-workers (*9*) and was termed DEAR (dipolar exchange-assisted recoupling). However, DEAR is neither an MAS method nor does it explicitly use the concept of recoupling. We have now generalized it for application to any kind of heteronuclear spin system under MAS. The requirements are that T_1 relaxation times of the heteronucleus are on the order of 1 s or less, which is the case for most quadrupolar nuclei, and that slow dynamics

[1] To whom correspondence should be addressed at Department of Chemistry, Iowa State University, Ames, IA 50011. Fax: 515-294-0105. E-mail: srohr@iastate.edu.

1090-7807/00 $35.00

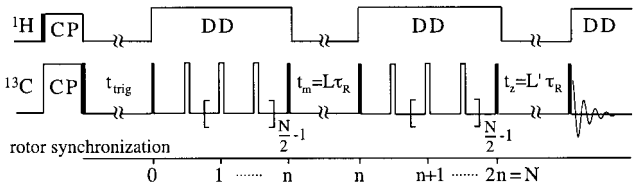

FIG. 1. Pulse sequence for the CODEX and RIDER experiments. In our experiments, the π-pulse trains (open bars) were phase-cycled according to the *xy*-4 scheme (*27*); for the phase cycling of the CP and the 90° pulses (solid bars), the reader is referred to the literature (*10, 11*).

or spin diffusion on the same time scale can be excluded. The pulse sequence is identical to that of the CODEX (centerband-only detection of exchange) experiment for characterizing slow dynamics (*10*). However, the mechanism of exchange by dipolar coupling to a relaxing heteronucleus is so different that we suggest a different acronym for the application presented here: RIDER, for relaxation-induced dipolar exchange with recoupling. It yields distance-dependent dephasing curves in close analogy to REDOR.

Under Theoretical Background, we give a detailed account of the spin dynamics under the S-L coupling with $S = \frac{1}{2}$, with $L = \frac{1}{2}$ or $L = 1$, and with T_1 relaxation during the mixing time. We present analytical solutions for the most important cases including isolated S-L spin pairs and rapidly rotating SL_3 moieties, as encountered in CD_3 groups. The possibility of extensions of the treatment to more complicated multispin systems and spins with $L > 1$ is indicated. We demonstrate the technique on L-alanine and d_3-methylmalonic acid.

PULSE SEQUENCE

The pulse sequence used is displayed in Fig. 1. It has been modified from the original CODEX experiment (*10*) by insertion of another *z*-filter, t_{trig}, after the cross polarization (CP) contact pulse to provide trigger time for rotor synchronization. In the original experiment, this was done before the CP, such that the minimum mixing time was at least as long as the contact pulse. This sequence is now suitable for cases where long CP times are needed and fast relaxation processes are to be monitored, calling for very short mixing times.

After CP, the first train of π-pulses recouples the heteronuclear S-L dipolar interaction and the S-chemical shift anisotropy (CSA). The S-magnetization modulated in this way is then subject to exchange processes during t_{m}. The readout pulse after the mixing time is phase-cycled to record the full stimulated echo after the second recoupling period. The stimulated echo will be reduced if processes during t_{m} hamper the exact refocusing of the interactions which were acting on S-spin transverse magnetization during the first recoupling period. This can be due either to reorientations of the interaction tensors during the mixing time or to changes in the coherence state of the spin system, as effected by homonuclear spin diffusion or relaxation processes. For CODEX, the reduction of the stimulated echo intensity due to slow reorientations of the CSA tensor is monitored. For the method presented here, relaxation of the L spin is the mechanism which causes the observed dephasing of the stimulated echo intensity, while slow motional processes and spin diffusion must be negligible.

In order to measure the dipolar dephasing for a given recoupling time, two experiments are performed. The *dephased* echo (S) is measured by choosing a long mixing time, $t_{\text{m}} = L\tau_{\text{R}}$, and a final *z*-filter time, $t_z = L'\tau_{\text{R}}$, long enough for the dephasing of unwanted coherences. The *undephased* echo, S_0, which serves as a reference, can be measured by choosing a very short mixing time, $t_{\text{m},0}$, which should be just one or a few rotation periods. The loss of S-spin magnetization due to relaxation is identical to the first experiment, if the overall periods of transverse and longitudinal relaxation are the same in both experiments. Therefore, the final *z*-filter time in the reference experiment, $t_{\text{z},0}$, is set so that $t_{\text{m},0} + t_{\text{z},0} = t_{\text{m}} + t_z$. The reference S_0 is thus used to correct for S-spin T_1 and T_2 relaxation and is the equivalent of the reference spectrum in a REDOR experiment, where the dephasing π-pulse on the L-spin is skipped to measure the undephased spectrum. The normalized dephasing calculated as $\Delta S/S_0 = 1 - S/S_0$ is then *only* dependent on the total recoupling time $N \cdot \tau_{\text{R}}$, the dipolar coupling to the L-nuclei, and the relaxation times of the L-nuclei. In cases where the heteronuclei in question are not 100% abundant, the intensity S_0 must be corrected accordingly.

THEORETICAL BACKGROUND

Throughout this section, we will assume the heteronuclear dipolar interaction to be the dominant interaction for the spectra. Due to the acquisition of the full stimulated echo any chemical shift evolution is compensated for by the pulse sequence (for details see (*11*)). The heteronuclear dipolar coupling Hamiltonian under MAS in the secular approximation reads

$$H^{(0)}_{\text{D},SL}(t) = 2d_{SL}(t)S_zL_z \qquad [1]$$

with the time-dependent dipolar coupling

$$d_{SL}(t) = \sum_{m=-2}^{2}\left[\sum_{m'=-2}^{2}\frac{1}{\sqrt{6}}A^{\text{C}}_{2,-\text{m}'}\mathcal{D}^{(2)}_{-\text{m}',-\text{m}}(\Omega_{\text{CR}})\right] \times e^{im\omega_{\text{R}}t}d^{(2)}_{-\text{m},0}(\beta_{\text{M}}). \qquad [2]$$

S and **L** represent the respective spin operators, β_{M} is the magic angle, and $\mathcal{D}^{(2)}_{\text{m},\text{m}'}(\alpha, \beta, \gamma)$ and $\text{d}^{(2)}_{\text{m},\text{m}'}(\beta)$ are the second-order full and reduced Wigner rotation matrices, respectively, for instance as given in (*12*). The $A^{\text{C}}_{2,-\text{m}'}$ are the spherical components of the dipolar interaction tensor $\mathbf{A}^{\text{C}}_2$ in the crystal frame, and Ω_{CR} denotes the set of Euler angles (α_{CR}, β_{CR}, γ_{CR}) which relate the crystal frame to the rotor frame. For the case of just one S-L pair, the internuclear vector is trivially assumed to be along the

z-axis of the crystal frame. In that case, the dipolar tensor is diagonal and symmetric in the crystal frame (which then coincides with the dipolar principal axes system). Thus, only $A^{C}_{2,0} = -\sqrt{6}\, D_{SL}$ contributes and only one term remains in the summation in square brackets. Also, $\mathcal{D}^{(2)}_{0,-m}(\Omega_{CR})$ does not depend on α_{CR}, which means that the powder average only has to be performed over $\beta_{CR} = \beta_{DR}$ (the azimuthal angle of the dipolar vector in the rotor frame) and $\gamma_{CR} = \gamma_{DR}$ (the initial rotor phase). The heteronuclear dipolar coupling constant (in rad/s) is given by

$$D_{SL} = -\frac{1}{\sqrt{6}} A^{C}_{2,0} = (\mu_0/4\pi)\gamma_S\gamma_L\hbar/r^3_{SL}. \qquad [3]$$

From Eq. [1], the average REDOR Hamiltonian for one rotor period of free evolution under the action of the refocusing π-pulses can be calculated:

$$\bar{H}_{SL}(\omega_R) = \frac{2}{\tau_R}\int_0^{\tau_R/2} H^{(0)}_{D,SL}(t)dt. \qquad [4]$$

Considering just one L-spin (z-axial symmetry in the crystal frame), the total phase acquired under recoupling for one rotor period is calculated to be (*13*)

$$\Phi = \frac{D_{SL}}{\omega_R} 2\sqrt{2}\sin(2\beta_{DR})\sin(\gamma_{DR}), \qquad [5]$$

where β_{DR} and γ_{DR} are now the Euler angles relating the dipolar vector to the rotor frame.

Coupling to $L = \frac{1}{2}$. To highlight the principles of the method, we shall first consider the simple case of an S-L pair with each of the nuclei being spin-$\frac{1}{2}$. In product operator notation (*14*), the density matrix after the first recoupling period acting on transverse x-magnetization before the flip-back pulse reads

$$\rho(\tfrac{1}{2}N\tau_R) = S_x\cos(\tfrac{1}{2}N\Phi) + 2S_yL_z\sin(\tfrac{1}{2}N\Phi). \qquad [6]$$

Both components of transverse S-magnetization and antiphase coherence are stored along z in subsequent scans. Thus, during t_m only the effect of L-spin T_1 relaxation has to be taken into account and the explicit calculation of the storage pulses is not necessary. S-spin T^S_1 or T^S_2 relaxation will not be considered, since the experiment is performed in such a way that the measured quantity $\Delta S/S_0$ will not depend on these, as a result of the division of the dephased signal by the reference intensity.

The operator L_z represents a nonequilibrium state and is thus subject to randomization by longitudinal relaxation according to $L_z \rightarrow L_z\exp(-t_m/T_1) \xrightarrow{t_m\to\infty} 0$. Throughout this paper, we will neglect any anisotropy of the T_1 relaxation, since the emphasis of this work is on the determination of dipolar coupling constants and internuclear distances. Nevertheless, in applications of RIDER for the study of relaxation processes of the heteronucleus, a better understanding of the influence of the T_1 anisotropy would be desirable. Apart from implications for the powder averaging, it may lead to the observation of nonexponential relaxation behavior (*15*).

Moreover, the treatment presented here is based on the assumption that the relaxation of the S_zL_z state (which is present during t_m) can be treated as a product of independently relaxing, pure S_z and L_z states. This is true if the SL dipolar coupling itself does not contribute to the relaxation to a large extent (due to its small size of 1 kHz and less, this can safely be assumed for the systems studied in this paper). Moreover, in the description of dipolar-mediated cross-relaxation (*16*) (i.e., NOE), the cross-relaxation rate of one spin is proportional to the expectation value of z-magnetization of the other spin. In the experiment, the phase cycle is designed in such a way that during t_m the S-magnetization is stored along z and $-z$ in alternate scans. This should largely cancel contributions from SL cross-relaxation to the polarization of the L-spins.

The density matrix after the second recoupling period (where the sign of the dipolar Hamiltonian is effectively inverted) is thus given by

$$\begin{aligned}\rho(N\tau_R) = {} & S_x\cos^2(\tfrac{1}{2}N\Phi) + 2S_yL_z\cos(\tfrac{1}{2}N\Phi)\sin(\tfrac{1}{2}N\Phi) \\ & + e^{-t_m/T_1}\Big(2S_yL_z\sin(\tfrac{1}{2}N\Phi)\cos(\tfrac{1}{2}N\Phi) \\ & + S_x\sin^2(\tfrac{1}{2}N\Phi)\Big). \end{aligned} \qquad [7]$$

After the final z-filter, only S_x (i.e., in-phase) components of transverse magnetization will be detected. Therefore, for vanishing mixing time the full initial S-spin signal is measured ($\cos^2 + \sin^2 = 1$). The powder-averaged dipolar dephased signal thus reads

$$\begin{aligned}\frac{\Delta S^{(L=1/2)}}{S_0}\left(t_m, N\right) &= 1 - \Big\langle \cos^2(\tfrac{1}{2}N\Phi) \\ &\quad + e^{-t_m/T_1}\sin^2(\tfrac{1}{2}N\Phi)\Big\rangle \\ &= 1 - \tfrac{1}{2}\Big\langle \cos(N\Phi) + 1 + e^{-t_m/T_1} \\ &\quad \times (1 - \cos(N\Phi))\Big\rangle \xrightarrow{t_m\to\infty} \\ &\quad \tfrac{1}{2} - \tfrac{1}{2}\langle\cos(N\Phi)\rangle \xrightarrow{N\to\infty} \frac{1}{2}. \end{aligned} \qquad [8]$$

For long mixing times, the $\sin^2$ component will not contribute

to the stimulated echo, and the result (last line) then represents a dephasing curve identical to the one measured in a REDOR experiment, but with the difference that the relative dephasing $\Delta S/S_0$ will not reach a final value of 1, but will be scaled down to $\frac{1}{2}$.

Coupling to L = 1. In this case, the calculation of the S-spin evolution under the S-L coupling is more involved. The **S** operators have to be split into two components—one component associated with the $|0\rangle_L$ eigenstate of the L-spin and another associated with the $|+1\rangle_L$ and $|-1\rangle_L$ states (*17*):

$$\rho(0) = S_x = S_x(\mathbf{1}_L - L_z^2) + S_x L_z^2, \qquad [9]$$

where the former component is invariant under the action of the Hamiltonian in Eq. [1], and the latter evolves with *twice* the coupling constant into in- and antiphase components according to

$$\rho(\tfrac{1}{2}N\tau_R) = S_x(\mathbf{1}_L - L_z^2) + S_x L_z^2 \cos(N\Phi) + S_y L_z \sin(N\Phi). \qquad [10]$$

Again, the storage pulses for the S-spins before and after the mixing time do not need to be considered explicitly. It seems tempting to conclude that for $L = 1$, with $\frac{1}{3}$ of the signal being invariantly coupled to $|0\rangle_L$, and $\frac{2}{3}$ of the magnetization being dephased according to Eq. [10] (in analogy to the $L = \frac{1}{2}$ case, Eq. [8]), the overall intensity of $\Delta S/S_0$ reaches only $1 - (\frac{1}{3} \cdot 1 + \frac{2}{3} \cdot \frac{1}{2}) = 33\%$. This is, however, not true, since the randomization of the L_z components during t_m also affects the $S_x(\mathbf{1}_L - L_z^2)$ component, which is invariant under dipolar coupling. In the Appendix, the relaxation behavior of the L_z and L_z^2 spin states is derived:

$$L_z \rightarrow L_z e^{-t_m/T_1^{app}} \xrightarrow{t_m \to \infty} 0 \qquad [11]$$

$$L_z^2 \rightarrow \tfrac{2}{3}\mathbf{1}_L - (\tfrac{2}{3}\mathbf{1}_L - L_z^2)e^{-3t_m/T_1^{SQ}} \xrightarrow{t_m \to \infty} \tfrac{2}{3}\mathbf{1}_L. \qquad [12]$$

From this, it is now possible to derive a correct qualitative description of the dephasing process for long recoupling and mixing times. It is clear that, after evaluation of the t_m-dependence in analogy to Eq. [7], one must regroup some of the product operators according to Eq. [12] before calculating the effect of the second recoupling period. The S_x component associated with $|0\rangle_L$, $S_x(\mathbf{1}_L - L_z^2)$, will thus relax to $S_x \frac{1}{3}\mathbf{1}_L$ for long mixing times. This coherence splits into yet another triplet (randomization upon relaxation during the mixing time), of which only one further $\frac{1}{3}$ remains invariant during the second recoupling period, while the rest acquires a cosine modulation with an average of zero, contributing $\frac{1}{9} \cdot 1$ to the signal in the long-time limit. Of the $\frac{2}{3}$ of the components associated with $|+1\rangle_L$ and $|-1\rangle_L$, a further $\frac{2}{3}$ will acquire an overall phase factor $\cos^2(N\Phi)$, resulting in a signal contribution of $\frac{2}{3}\frac{2}{3} \cdot \frac{1}{2}$ in the long-time limit. The plateau value of $\Delta S/S_0$ for infinite t_m and infinite $\tau_{rcpl} = N\tau_R$ is thus $1 - S_\infty/S_0 = 1 - (\frac{1}{3}\frac{1}{3} \cdot 1 + \frac{2}{3}\frac{2}{3} \cdot \frac{1}{2}) = 66\%$.

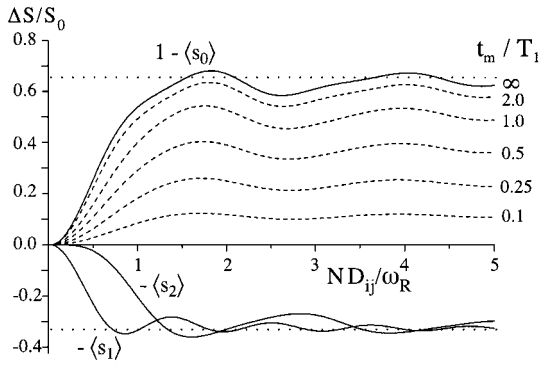

FIG. 2. Theoretical RIDER buildup curves for $L = 1$ as calculated from Eq. [13]. These curves represent master curves in a sense that the x-axis scales with the product of the dipolar coupling constant and the recoupling time $2\pi N/\omega_R$. The solid lines represent the powder-averaged coefficients $(1 - \langle s_0\rangle)$, $-\langle s_1\rangle$, and $-\langle s_2\rangle$, whereas the dashed lines are linear combinations of these for the indicated ratios of t_m/T_1^{SQ} and for $T_1^{DQ} \rightarrow \infty$.

Following the procedure outlined under Coupling to $L = \frac{1}{2}$, the full time dependence of the measured signal can be derived. The powder-averaged t_m- and N-dependent dephasing for S coupled to one $L = 1$ spin is calculated to be

$$\frac{\Delta S^{(L=1)}}{S_0}(t_m, N) = 1 - \left\langle s_0(N) + s_1(N)e^{-t_m/T_1^{app}} + s_2(N)e^{-3t_m/T_1^{SQ}} \right\rangle, \qquad [13]$$

where

$$s_0(N) = \tfrac{1}{9}(3 + 4\cos(N\Phi) + 2\cos(2N\Phi)),$$

$$s_1(N) = \tfrac{1}{9}(3 - 3\cos(2N\Phi)),$$

$$s_2(N) = \tfrac{1}{9}(3 - 4\cos(N\Phi) + \cos(2N\Phi)),$$

and

$$T_1^{app} = T_1^{SQ}T_1^{DQ}/(T_1^{DQ} + 2T_1^{SQ}). \qquad [14]$$

As required, for $t_m = 0$ the three coefficients $s_i(N)$ add up to unity to give the full stimulated echo. For longer mixing times, dephasing curves are obtained whose plateau values for long recoupling times ($N \rightarrow \infty$) depend on the single- and double-quantum relaxation times of the L nucleus.

In Fig. 2, some buildup curves are depicted for different values of t_m/T_1 (for the case of $T_1^{DQ} \rightarrow \infty$). In the limit of $t_m \rightarrow$

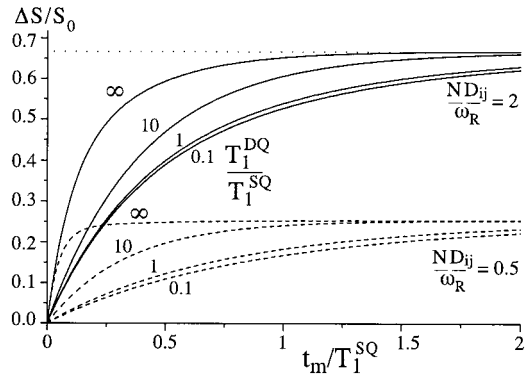

FIG. 3. Theoretical RIDER relaxation curves for spin $L = 1$ as calculated from Eq. [13], depending on the ratio of t_m/T_1^{SQ} for the cases of $ND_{SL}/\omega_R = 0.5$ (dashed lines) and $ND_{SL}/\omega_R = 2.0$ (solid lines). The numbers indicated at the curves are the corresponding ratios of T_1^{DQ}/T_1^{SQ}.

∞, the dephasing curve is $\langle 1 - s_0(N)\rangle$, with a plateau value of $1 - \frac{3}{9} = 66\%$. It should be noted that the position of the first maximum of the buildup curves does not change considerably as a function of the two T_1 relaxation times, if the mixing time is sufficiently long (at least $2T_1^{SQ}$); thus the dipolar coupling constant can be determined quite accurately without exact knowledge of the ratio of T_1^{SQ} and T_1^{DQ}.

To further probe the effects of T_1^{SQ} and T_1^{DQ} on the dephasing curve, the changes of the relative dephasing with the mixing time for various ratios T_1^{DQ}/T_1^{SQ} are explored in Fig. 3. The dependences on the relaxation times in the exponential factors are weighted by the coefficients s_1 and s_2, the ratio of which for a given recoupling time is different for the two different recoupling times indicated (see Fig. 2). Since the dependence of the signal on the double-quantum relaxation time resides only in the s_1 term, it is possible to extract both relaxation times from measurements of relaxation curves at suitably chosen recoupling times.

The structure of Eq. [13] suggests an efficient way for a numerical fitting procedure of experimental data. The dependence on the recoupling time, and thus on the dipolar coupling constant, resides in the three coefficients $s_i(N)$. Since all three scale with the ratio of ND_{SL}/ω_R (Eq. [5]), powder-averaged master curves can be calculated for each single coefficient. Derivatives of these master curves with respect to the dipolar coupling can be obtained by interpolation, and the derivatives with respect to the relaxation times can be calculated analytically. These derivatives are needed for gradient-based χ^2-minimization algorithms such as the widely used Levenberg–Marquardt method. Such a least-squares fitting procedure will thus yield the relaxation times and a stretching factor for the ratio ND_{SL}/ω_R, from which, taking into account the simulation parameters of the master curves, the dipolar coupling can be obtained.

Couplings to multiple L-spins. The treatment of the couplings of an S-spin to multiple L-spins for the REDOR experiment has already been published (*13*). In short, since the heteronuclear dipolar coupling Hamiltonians all commute with each other, $[\bar{H}_{SL_i}, \bar{H}_{SL_j}] = 0$, the dipolar dephasings for all individual SL_i-pairs can be evaluated *independently,* resulting in a dephasing signal that is the *product* of individual pair contributions. This holds equally well for the RIDER experiment. Homonuclear couplings among the L-spins are assumed not to contribute to a first approximation, because only longitudinal components of L-magnetization are involved. Also, in weakly coupled spin systems, this interaction should largely be averaged out by the MAS. However, in the case of different chemical shifts and rather strong homonuclear couplings among the L-spins, as for instance encountered in ^{19}F systems, the noncommutation of L_z and $\bar{H}_{LL} \propto T_{2,0}$ leads to deviations from the analytically tractable case (*13*). For RIDER, homonuclear coupling among the S-spins is also of no importance, since the exclusion of spin diffusion restricts the application of the method to the case of high isotopic dilution of the S-spins. The dephased signal is therefore calculated as

$$\frac{\Delta S}{S_0}(t_m, N) = 1 - \left\langle t\prod_{i=1}^{n_L} f_i \right\rangle, \qquad [15]$$

where the individual pair contributions f_i are the terms subject to the powder average in Eqs. [8] and [13]. It should be emphasized that the powder average must be evaluated *after* the multiplication of the individual dephasing factors. Also, the dipolar phases Φ_i are now mutually dependent via the geometry of the spin system. Consequently, Eq. [5] cannot be applied anymore, since the individual S-L pair vectors cannot all be assumed to coincide with the z-axis of the crystal frame. Rather, another transformation of these individual pair vectors from their dipolar PAS to the crystal frame must be introduced before powder-averaging the product dephasing over Ω_{CR}. A treatment of Φ_i as a function of individual pair vector orientations has also been given by Goetz and Schaefer (*13*). If coordinates of the various nuclei rather than Euler angles are known, it is more convenient to calculate the spherical components of the dipolar tensors directly and use Eq. [2].

When couplings to a methyl (or CD_3) group are to be considered, Eq. [15] can be simplified even further. In essence, methyl groups undergo fast three-site jumps at ambient temperature, possibly with some orientational distribution around the three sites (*18*). Therefore, the three heteronuclear couplings involved have an identical dependence upon position, such that

$$\frac{\Delta S^{Me}}{S_0}(t_m, N) = 1 - \langle f_{Me}^3 \rangle. \qquad [16]$$

The spatial part of the dipolar coupling is described by a symmetric second-rank tensor. The average of such second-rank tensors undergoing fast symmetric jumps with three or more positions around a specified axis is again represented by

a uniaxial tensor with its symmetry axis along the rotation axis (*19*). Therefore, the acquired dipolar phase for a single S-L pair with S located on the rotation axis can again be calculated using Eq. [5], but with a modified dipolar coupling constant (*20*)

$$D_{SL}^{\text{app}} = D_{SL}\,\tfrac{1}{2}(3\cos^2\theta - 1), \qquad [17]$$

where θ is the angle between the S-L internuclear vector and the methyl rotation axis. For S-spins located off the rotation axis, Eq. [16] still holds, but the averaged dipolar tensor (simply calculated as the average of the three different $\mathbf{A}_2^C$) will then be asymmetric. Consequently, it will depend explicitly on the position of the three individual L-sites relative to the S-spin, yielding a more complicated formula for D_{SL}^{app}. In the off-axis case, Eq. [17] represents a good approximation only when $r_{SL} \gg r_{LL}$, or for small displacements of the S-spin from the rotation axis, i.e., corresponding to very small asymmetry parameters.

For the case of $t_m \to \infty$, the N-dependent dephasing for the CD_3 group is calculated from Eqs. [13] and [16] to be

$$\frac{\Delta S}{S_0}^{\text{CD}_3}\left(N\right) = 1 - \langle s_0^3(N)\rangle$$
$$= \frac{1}{9^3}\Big\langle 588 - 252\cos(N\Phi) - 180\cos(2N\Phi)$$
$$- 100\cos(3N\Phi) - 42\cos(4N\Phi)$$
$$- 12\cos(5N\Phi) - 2\cos(6N\Phi)\Big\rangle. \qquad [18]$$

The dephased signal thus reaches a plateau of 588/729 = 80.66%.

EXPERIMENTAL

Instrumentation. The experiments were performed on a Bruker DSX 300 spectrometer operating at 300.13 MHz for ^{1}H and 75.49 MHz for ^{13}C. A commercial Bruker double-resonance MAS probe for rotors of 7-mm diameter was used. The 90° pulse lengths on both channels were about 3.5–4.5 μs, corresponding to B_1 nutation frequencies of 71–56 kHz. The proton B_1 field was increased during recoupling and acquisition by at least 10 kHz. For all reported experiments, the spinning speed used was 6 kHz, and the CP contact time was 500 μs. The first z-filter delay, t_{trig}, as well as $t_{\text{m},0}$ and $t_{\text{z},0}$, was set to 1 ms.

Samples. The RIDER measurements were carried out on commercially available L-alanine, with ^{14}N in 99.6% natural abundance, and on CD_3-labeled methylmalonic acid (>98% D), which was purchased from C/D/N Isotopes, Inc., and used without further purification. Owing to the favorable relaxation behavior of the methyl protons in L-alanine, the recycle time was 1 s in this case, whereas for the d_3-methylmalonic acid scans were repeated every 30 s. Typically, 512 scans were accumulated for the L-alanine and 128 scans for d_3-methylmalonic acid. For the latter sample, arcing in the probe limited the B_1 field strengths to about 55 kHz, corresponding to 4.5-μs pulses. For the same reason, the acquisition time was limited to about 10 ms, making quite large line broadening necessary. This explains the relatively poor signal-to-noise ratio and resulting large error bars in Fig. 7.

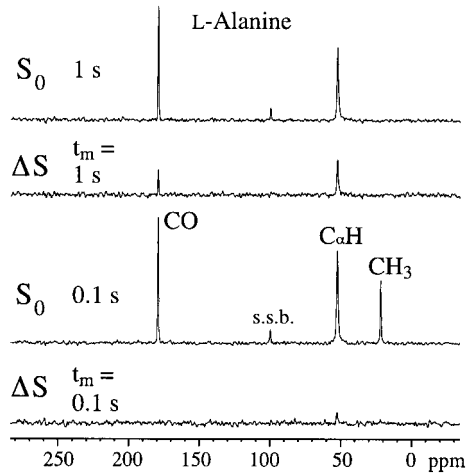

FIG. 4. RIDER reference (S_0) and difference (ΔS) spectra of L-alanine for a total recoupling time of 26 τ_R = 4.33 ms, using two different mixing times t_m = 0.1 s and t_m = 1 s. Spinning sidebands of the CO carbon are denoted by s.s.b.

RESULTS AND DISCUSSION

^{13}C–^{14}N distances in L-alanine. In Fig. 4, RIDER difference spectra (ΔS) for a relatively long recoupling time and two different mixing times, along with the corresponding reference spectra, are displayed. At short mixing times, the exchange due to ^{14}N relaxation is minor. Therefore, only the C_α peak is visible, whereas at longer mixing times the carbonyl signal becomes observable as well. Moreover, the intensity of the C_α signal (to be interpreted relative to the corresponding reference intensity, S_0) increases considerably. A basic limitation of the technique becomes obvious by comparing the two reference spectra. At mixing times as short as 1 s, the signal from the methyl carbon is already completely relaxed, which means that the distance information for this site cannot be determined with this method. To obtain distance information between two types of nuclei, the relaxation time of the detected nucleus should be at least equal to the relaxation time of the passive spin.

The dipolar coupling constants can be determined most accurately by measuring the normalized dephasing, $\Delta S/S_0$, as a function of recoupling time and fitting the data according to Eq. [13], following the procedure outlined under Theoretical Background. The buildup data for two different mixing times are presented in Fig. 5. The data points were fit to Eq. [13],

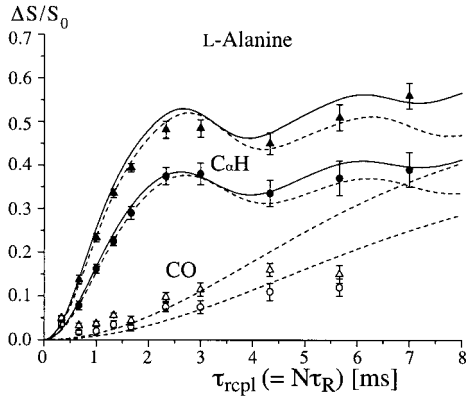

FIG. 5. RIDER buildup curves of L-alanine as a function of the recoupling time, using mixing times of 800 (triangles) and 400 ms (circles). Solid symbols denote data for the C_α resonance, open symbols are from the CO signal. The dashed lines are the best-fit spin pair curves using Eq. [13], solid lines represent simulations based on Eq. [15], considering the C_α–N pair and the 12 closest N atoms from neighboring molecules (up to a CN distance of 6 Å), the positions of which were taken from the crystal structure (*23, 24*). The relaxation times for these simulations were taken from the data displayed in Fig. 6.

assuming that the contribution from ^{14}N DQ relaxation is insignificant (i.e., $T_1^{app} = T_1^{SQ}$), which has previously been shown to be a valid assumption for L-alanine (*21*). For the C_α carbon, the agreement between the experimental data and the fit (dashed lines) is good. The dipolar coupling constant is determined to be 630 ± 40 Hz, which corresponds to a C_α–N distance of 1.51 ± 0.03 Å (*22*). This agrees well with previous NMR measurements (*9*). The value should be compared with $r_{C_\alpha N} = 1.489$ Å obtained from neutron and low-temperature X-ray diffraction data (*23, 24*). Small discrepancies between distances measured by NMR and scattering methods are commonly encountered and can be explained by different averaging of fast vibrational and librational motions (*25*).

Deviations from the theoretical behavior are observed for longer recoupling times. This can straightforwardly be explained by the fact that we did not dilute the spin pairs in question. As a result, for large τ_{rcpl} couplings to remote spins contribute to the signal appreciably. The last one or two data points of each series were actually excluded from the fit in order to achieve a good agreement with the spin pair approximation. It is common practice in experiments like REDOR to analyze only the initial buildup behavior, which is largely independent of the remote couplings. If an estimate of the influence of remote couplings is not available, isotopic dilution is necessary.

In the graph we also included simulated dephasing curves (solid lines) based on the crystal structure of L-alanine (*23, 24*), which, apart from the primary C_α–N pair, also take into account the 12 closest ^{14}N-spins from neighboring molecules. The reason for the shift of the maxima of these curves relative to the fits, and thus the difference in experimentally determined and expected dipolar couplings, has already been explained above. Apart from that, these simulations can indeed account for the higher dephasing measured at longer recoupling times. The plateau values given under Theoretical Background are strictly valid only for the cases of completely isolated spin pairs or SL_3 groups. In a real system, the normalized dephasing will always reach a value of 1 (complete dephasing) in the limit of infinite recoupling time. From the simulations, it is, however, obvious that satisfactory results *can* be obtained in systems without isotopic dilution, if one restricts the analysis to reasonably short recoupling times. As is obvious, the multispin simulation and the fit assuming an isolated spin pair agree well even beyond the first maximum of the buildup curve.

As already mentioned, the signal from the methyl group could not be evaluated. Also, the agreement between the data for the carbonyl carbon and the theoretical curves is somewhat poor. We believe that this problem arises primarily because for the calculation of $\Delta S/S_0$, due to signal-to-noise considerations, only centerband intensities were used, whereas at a spinning speed of 6 kHz, owing to the rather large CSA of a carbonyl group, weak spinning sidebands were still visible. The intensity distribution between the centerband and first-order sidebands was different between the dephased and the reference spectra in some cases, which was possibly due to timing imperfections of the rotor trigger. In light of this kind of problem, it is advisable to work at spinning frequencies which are large enough to completely average out the CSA, i.e., in a regime where no spinning sidebands appear. Alternatively, TOSS detection can be implemented in CODEX/RIDER experiments (*11*). Nevertheless, as shown in Table 1, the distance derived from the fit again agrees with the expected value.

The height of the first maxima and the plateau values of the best-fit curves in Fig. 5 depend on the two relaxation times T_1^{SQ} and T_1^{DQ}. Since a fit of buildup curves alone does not yield reliable results for these two times (as shown, the expected plateau is often increased due to the influence of remote spins), it is advisable to record relative dephasings for various recoupling times as a function of the mixing time and fit these to Eq. [13], but with fixed coefficients $\langle s_i \rangle$. The $\langle s_i \rangle$ can be calculated for any recoupling time once the dipolar coupling constant is known. It is advisable to measure these relaxation curves at moderate recoupling times, in order to keep the perturbing influence of remote spins small. The experimental data along with the fits are displayed in Fig. 6, where it is shown that a single-quantum relaxation time $T_1^{app} = T_1^{SQ} = 0.9903 \pm 0.033$

TABLE 1
Experimentally Observed and Expected Dipolar Couplings and Bond Lengths for L-Alanine

	NMR		From crystal structure[a]	
	$D_{CN}/2\pi$ (Hz)	r_{CN} (Å)	$D_{CN}/2\pi$ (Hz)[b]	r_{CN} (Å)
C_α	630 ± 40	1.51 ± 0.03	661	1.489
CO	130 ± 20	2.56 ± 0.13	144	2.473

[a] As determined by neutron scattering (*23*).
[b] Calculated from Eq. [3].

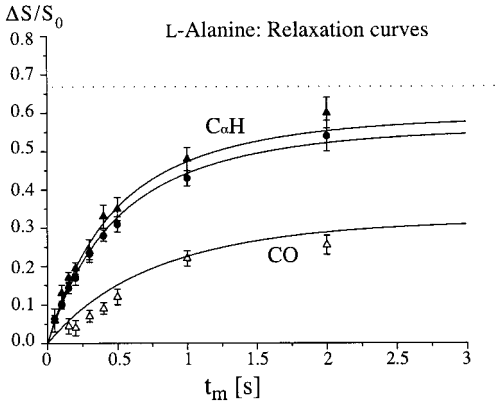

FIG. 6. RIDER relaxation curves of L-alanine, using recoupling times of 10 τ_R = 1.67 ms (triangles) and 26 τ_R = 4.33 ms (circles). Solid symbols denote data for the C_α resonance; open symbols are from the CO signal. The averaged best-fit curves (solid lines) using Eq. [13] with fixed coefficients $\langle s_i \rangle$ (taken from the results of the fits in Fig. 5) were calculated for $T_1^{SQ} = 0.903 \pm 0.033$ s and $T_1^{DQ} = \infty$.

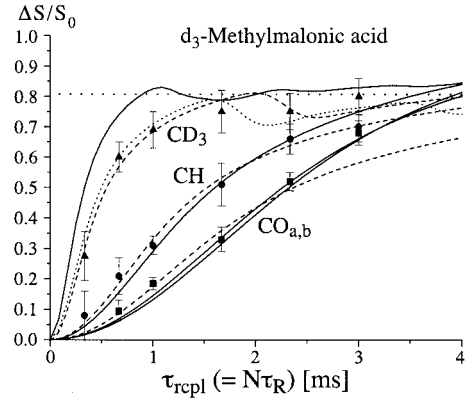

FIG. 7. RIDER buildup curves of d_3-methylmalonic acid for a mixing time of 100 ms. Triangles, circles, and squares represent the experimental results for the CD_3, the CH, and the CO resonances, respectively. The best-fit curves, based on Eq. [18] in the limit of long mixing times, are indicated by dashed lines. The solid lines are simulations based on the average dipolar coupling tensors of the nine closest deuteron triplets (up to a CD distance of 6 Å) as taken from the X-ray crystal structure (*26*), and include a finite mixing time and the relaxation time determined by fitting the data in Fig. 8. There are two curves for the two inequivalent CO sites in the crystal. The dotted line is a four-spin simulation based on a more realistic tetrahedral arrangement of the CD_3 with a distance of r_{CD} = 1.09 Å, also based on the experimentally determined relaxation time, $T_1^{app} = T_1^{SQ}$.

s, and $T_1^{DQ} = \infty$, agrees with the measurements. It was not possible to reliably fit the data with the two relaxation times as independent parameters; it can merely be stated that a χ^2-analysis of the data indicated that T_1^{DQ} is at least five times larger than T_1^{SQ}. These results are in good agreement with the work of Naito *et al.* (*21*), where single-crystal static ^{13}C 2D exchange measurements were analyzed. The value due to Frydman and co-workers of $T_1^{SQ} = 0.090 \pm 0.06$ s (*9*), as determined using the DEAR experiment, does, however, differ significantly.

In the analysis outlined above, an interdependence of the fits of the buildup and the relaxation data becomes apparent. This arises because in the fits of the buildup curves for the determination of the dipolar coupling, the dependence on the relaxation times could not be neglected, since the mixing times were only on the order of T_1^{SQ}. Thus, a χ^2-analysis was required to ensure the reliability of the results for the dipolar coupling and the relaxation times. It shall again be mentioned that the determination of the dipolar coupling constants is most accurate for long mixing times, i.e., $t_m > 2T_1^{SQ}$. Then, the dependence of the result on the relaxation times is negligible. If the sample is not isotopically diluted, the influence of remote spins can be minimized by restricting the analysis to the initial rise of the buildup data and the measurement of relaxation curves to moderate recoupling times.

^{13}C–^2H distances in d_3-methylmalonic acid. Relatively well-isolated deuterated methyl groups represent a good system for testing the dephasing behavior in the RIDER experiment for the case of couplings to multiple spins. The data for our model compound, along with best-fit and simulated curves, are displayed in Figs. 7 and 8. A comparison between measured and expected values for the coupling constants is presented in Table 2. When simulating the dephasing curves based on crystal structure data, the rapid three-site jumps of methyl deuterons were generally accounted for by arithmetically averaging the five spherical components $A^C_{2,m}$ of the three different dipolar coupling tensors and assigning the average tensor to each of the CD dipolar pairs. Also, all dipolar coupling constants and recoupling times were scaled by factors of 0.25 and 4, respectively, in order to obtain more points for the curves.

The fits (dashed lines) in Fig. 7 are based on Eq. [18], i.e., on the assumption of complete relaxation of the deuterons.

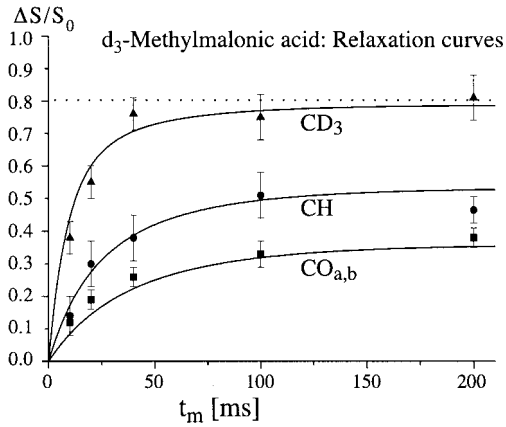

FIG. 8. RIDER relaxation curves of d_3-methylmalonic acid for a recoupling time of 10 τ_R = 1.67 ms. Triangles, circles, and squares represent the experimental results for the CD_3, the CH, and the CO resonances, respectively. The fits were performed using Eq. [16] under the assumption of negligible DQ relaxation. The result of the fits (solid lines) are plotted for the average $T_1^{app} = T_1^{SQ} = 56 \pm 14$ ms.

TABLE 2
Experimentally Observed and Expected Apparent Dipolar Couplings and Bond Lengths for d_3-Methylmalonic Acid

	NMR		From crystal structure[a]			Idealized CD_3 group[b]		
	$\lvert D_{CD}^{app}\rvert/2\pi$ (Hz)	r_{CD} (Å)	$D_{CD}^{app}/2\pi$ (Hz)[c]	η^c	r_{CD} (Å)	$D_{CD}^{app}/2\pi$ (Hz)[c]	η^c	r_{CD} (Å)
CD_3	966 ± 198	1.17 ± 0.08[d]	1625	0.59	1.117 0.931 1.162	−1193	0.0	1.09[e]
CH	348 ± 38	2.064 ± 0.08[f]	−323	0.15	2.121 2.043 2.170	−302	0.0	2.165
CO	224 ± 22	—	−162/−158[g]	0.17/0.11	2.69/2.68 3.23/2.78 2.72/3.51	−156/−148	0.05/0.09	2.75/2.75 3.38/2.86 2.59/3.49

[a] As determined by X-ray scattering (*26*).
[b] Assuming tetrahedral arrangement within the CD_3 and the carbon skeleton from the crystal structure.
[c] Calculated from the average dipolar tensor of the three proton positions.
[d] Calculated from Eqs. [3] and [17], assuming $\theta = 109.5°$.
[e] Distance usually found for methyl groups by neutron scattering, e.g., for L-alanine (*23*).
[f] Calculated from Eqs. [3] and [17], assuming $\theta = 28.4°$.
[g] Two inequivalent positions in the crystal.

Apart from deviations at long mixing times, the agreement with the experiment is good. In particular, the predicted plateau value of about 81% is confirmed. For a quantitative comparison with a simulation based on the crystal structure, neutron scattering results would be desirable, since they locate the protons reliably. Unfortunately, we had only data from X-ray scattering with which to compare the NMR results (*26*). The shortcomings of X-ray scattering for the exact localization of protons become obvious by comparing the experimental NMR data with the simulated dephasing curve for the CD_3 signal (upper solid line). The curve rises considerably faster and reaches a first maximum which is higher than theoretically expected. As can be seen in Table 2, the average dipolar coupling tensor for the three deuteron sites in the X-ray structure has an asymmetry parameter of $\eta = 0.59$ and a rather large positive apparent dipolar coupling constant (from Eq. [17], with θ being close to the tetrahedral angle, a negative sign would be expected). This means that the three sites are not equivalent in the X-ray structure and the local C_3 symmetry is apparently broken. One of the three distances is stated to be even shorter than 1 Å (see Table 2). Neutron scattering has shown that methyl groups in L-alanine and many other molecules possess a nearly tetrahedral symmetry, with a CH distance of 1.09 Å (*20*). Thus, dipolar coupling tensors calculated from such an arrangement of deuterons, with the carbon skeleton still taken from the X-ray data, represent a much better structural model. The dotted line in Fig. 7 is calculated from this model, the deviation now being within the expected range for differences between scattering and NMR distances.

The data for the CH and CO groups suggest higher coupling constants than those calculated from the idealized spin pair model. This is again due to the influence of the deuteron triplets of neighboring molecules, eight of which are accounted for in the simulated curves (solid lines) of Fig. 7. For longer distances, the poor localization of the protons by X-ray scattering becomes less significant, and these curves are seen to fit the data very well. The CH–D distance as determined from the fit on the basis of the idealized model (assuming $\theta = 28.4°$) is still within 5% of the expected value. Since the CO carbon is located off-axis from the methyl group, it is not possible to derive a unique distance from the apparent dipolar coupling constant (the motionally averaged dipolar tensor is now asymmetric). Also, the deviation of the measured coupling constant from each of the two values for the idealized spin pair model (which takes into account the two inequivalent CO sites in the crystal) is quite large in that case, again as a consequence of couplings to neighboring molecules.

The mixing-time-dependent data in Fig. 8 have again been fitted under the assumption of negligible DQ relaxation. In this case, this was merely due to the signal-to-noise ratio, which did not permit a reliable fit of both times. Deviations are observed, and T_1^{DQ} might thus be important, but more accurate data would be needed for a closer investigation. A value of $T_1^{SQ} = 56 \pm 14$ ms was obtained by fitting the data according to Eqs. [13] and [16], i.e., considering the powder average of all mixed products $\langle s_i s_j s_k \rangle$ with the appropriate exponential factors. In all but one of these contributions, t_m/T_1^{SQ} occurs with a prefactor >1, which actually explains the good agreement of the buildup data (acquired with $t_m \approx 2T_1$) with the theoretical curves for the limit of long relaxation times. Deviations between the master curves for the two cases of $t_m = 2T_1$ and $t_m = \infty$ are within 2%.

CONCLUSIONS

The RIDER experiment represents a promising new tool for quantitative distance measurements between unlike spins in solids, where one of the two spins is not irradiated at all. Thus, for distance measurements between ^{13}C or ^{29}Si and other heteronuclei, only double-resonance equipment is needed. The unspecific nature of the experiment might at first seem to be a serious limitation; nevertheless, we expect a wide applicability, since, first, it is usually possible to chemically control the isotope composition of the investigated compound, and, second, the T_1 relaxation times of various NMR-active nuclei differ by orders of magnitude, e.g., in ^{29}Si-containing systems, the ^{29}Si T_1 is usually so long that dipolar couplings to ^{29}Si as the L-spin do not play a role within experimentally relevant mixing times.

Compared to REDOR or REAPDOR, the intrinsic loss of 50% of the signal due to the alternating acquisition of the *x*- and *y*-components in subsequent scans represents a serious drawback, which is, however, at least partially compensated by the considerably higher sensitivity of the double-resonance probe heads used for RIDER compared to the triple-resonance probes needed to conduct the corresponding REDOR or REAPDOR measurements.

Moreover, the theoretical framework used to describe and model the measured data is quite straightforward, and no empirical factors have to be included in order to account for instabilities of the spectrometer with respect to the excitation of quadrupolar nuclei. Such problems usually arise in REAPDOR experiments, where it is often unavoidable to perform a calibration in order to extract the distance information (*8*). For the case of RIDER, we have shown that the data measured for the two compounds, L-alanine and d_3-methylmalonic acid, can be described *quantitatively* by using the crystal structure of these compounds and the longitudinal relaxation times determined from the RIDER experiment itself. Even though the measurements presented here were not particularly suited for an in-depth exploration of relaxation processes in quadrupolar nuclei, RIDER shows promise for such applications; in particular, higher quantum relaxation cannot be assessed using classical methods like inversion recovery.

Among the most basic limitations of the technique is that the T_1 relaxation time of the observed nucleus must be *at least* of the same order of magnitude as T_1 of the passive spin. This, however, is the case for almost all ^{13}C- and ^{29}Si-containing systems.

Another serious restriction is the requirement that slow dynamics (and spin diffusion) has to be excluded, since the stimulated echo at the end of the second recoupling period is reduced not only by heteronuclear dipolar dephasing, as described here, but also by changes in the segmental orientation or by magnetization exchange with neighboring spins (*11*). By conducting experiments at different temperatures or B_0 field strengths, it should be possible to distinguish between dephasing due to reorientations, spin diffusion, and relaxation-induced dipolar exchange: In the slow-motion limit of relaxation, the T_1 relaxation times decrease with increasing temperature, while reorientation speeds up and spin diffusion remains mostly unchanged. The correlation time of reorientations is field-independent, and the time dependence of spin diffusion nearly so, while T_1 relaxation times change significantly with B_0. Also, the dephasing due to CSA-related mechanisms (reorientations and spin diffusion) scales with B_0 as a function of the recoupling time, whereas for dipolar exchange the buildup curves are independent of B_0 in the limit of complete relaxation of the L-spin.

In conclusion, we expect that the RIDER experiment will open up new experimental possibilities, especially in laboratories where triple-resonance equipment is not yet available or where relaxation properties of quadrupolar nuclei are to be investigated.

APPENDIX

In order to derive the relaxation behavior of the operators L_z and L_z^2 for the case of $L = 1$, a connection must be established between the classical picture of relaxing expectation values of magnetization and the quantum statistical picture as represented by the product operators. To this purpose, we employ the concept of polarization operators (*17*). In the energy basis, the matrix representation of each of these operators has one nonzero entry, on the diagonal, representing the population of the associated spin state. These operators are the longitudinal equivalents of the single-transition shift operators L^+ and L^-, which each describe a single complex off-diagonal (transverse) mode of coherence. The complete set of these operators forms a basis set for the representation of the density operator ρ. A transformation into this representation is well suited to describe relaxation, because these processes can generally connect any two matrix elements of ρ. Mathematically, the simplicity of this description is due to the fact that the matrix representation of the relaxation superoperator $\hat{L}$ in this basis (the so-called Redfield Matrix **R**) has a block diagonal structure.

For a spin-1 system, one defines

$$L^{[+1]} = \tfrac{1}{2}(L_z^2 + L_z) \qquad [19]$$

$$L^{[0]} = \mathbf{1} - L_z^2 \qquad [20]$$

$$L^{[-1]} = \tfrac{1}{2}(L_z^2 - L_z). \qquad [21]$$

The L_z and L_z^2 operators can thus be written as linear combinations,

$$L_z = \sum_{m=-1}^{+1} p_{L_z}^{(m)}(0)\, L^{[m]} \qquad [22]$$

$$L_z^2 = \sum_{m=-1}^{+1} p_{L_z^2}^{(m)}(0)\, L^{[m]}, \qquad [23]$$

where $\vec{p}$ are vectors with components of individual populations. These can be visualized as representing classical magnetizations associated with the three spin states. In the single-transition operator basis, the time dependence upon relaxation is, as required within the Schroedinger picture, contained solely in the coefficients $p^{(m)}(t_m)$. Using the definitions of the polarization operators (Eqs. [19]–[21]), we arrive at the desired representation of the z-operators in terms of populations:

$$\vec{p}_{L_z}(0) = (+1, 0, -1)^T \quad [24]$$

$$\vec{p}_{L_z^2}(0) = (+1, 0, +1)^T. \quad [25]$$

Longitudinal relaxation leads to the randomization of the components of these vectors. Considering the T_1 relaxation phenomenologically in terms of the redistribution of polarization between energy levels, the time dependence of $\vec{p}(t_m)$ during relaxation is described by $\dot{\vec{p}} = \mathbf{K}\vec{p}$, where $\mathbf{K}$ is the exchange matrix characterizing the relaxation process (*21*). For spin-1 relaxation,

$$\mathbf{K} = \begin{pmatrix} -a-b & a & b \\ a & -2a & a \\ b & a & -a-b \end{pmatrix}. \quad [26]$$

The coefficients $a = 1/T_1^{SQ}$ and $b = 1/T_1^{DQ}$ represent the single- and double-quantum relaxation rates, respectively (*21*). The solution

$$\vec{p}(t_m) = e^{\mathbf{K}t_m}\vec{p}(0) \quad [27]$$

can be obtained by diagonalization of the $\mathbf{K}$-matrix. The matrix representation of $\exp(\mathbf{K}t_m)$ is given in (*21*) and is reproduced here for convenience.

$$e^{\mathbf{K}t_m} = \frac{1}{6}\begin{pmatrix} 2 + e^{-3at_m} + 3e^{-at_m-2bt_m} & 2 - 2e^{-3at_m} & 2+e^{-3at_m} - 3e^{-at_m-2bt_m} \\ 2 - 2e^{-3at_m} & 2 + 4e^{-3at_m} & 2 - 2e^{-3at_m} \\ 2 + e^{-3at_m} - 3e^{-at_m-2bt_m} & 2 - 2e^{-3at_m} & 2 + e^{-3at_m} + 3e^{-at_m-2bt_m} \end{pmatrix} \quad [28]$$

Evaluating the t_m dependence of the polarization vectors, and using $\vec{p}_1 = (+1, +1, +1)^T$, the "time dependence" of the z-operators according to Eqs. [22] and [23] is calculated to be

$$L_z \xrightarrow{\mathbf{K}t_m} L_z e^{-(a+2b)t_m} \quad [29]$$

$$L_z^2 \xrightarrow{\mathbf{K}t_m} \tfrac{2}{3}\mathbf{1} - (\tfrac{2}{3}\mathbf{1} - L_z^2)e^{-3at_m}. \quad [30]$$

These relations are to be understood in the same sense as in product operator theory, where the arrow is a shorthand notation to describe the time evolution in terms of the application of a unitary transformation superoperator as derived from the Liouville–von Neumann equation. Here, however, the time evolution under longitudinal relaxation is not described by a unitary transformation, as is clear from the nonconservation of the trace. Also, these relations only hold in the case of pure relaxation, with time evolution due to internal Hamiltonians of the system being excluded.

The treatment presented here can directly be extended to spins with $L > 1$, although the amount of algebra involved in solving $\exp(\mathbf{K}t_m)$ may then call for some approximations, such as neglecting higher quantum relaxation rates. It is interesting to note that the longitudinal relaxation time, measured as the decay time constant of z-magnetization (Eq. [29]), is equal to the single-quantum longitudinal relaxation time only in the case of insignificant double-quantum relaxation. Otherwise, an apparent $T_1^{app} = T_1^{SQ}T_1^{DQ}/(T_1^{DQ} + 2T_1^{SQ})$ is observed.

ACKNOWLEDGMENTS

Financial support was provided by NSF (Grant DMR-97 03916). KS thanks the German Academic Exchange Service (DAAD) for a short-term stipend and the research group of KSR for providing a friendly and productive working atmosphere during the Summer of 1999 in Amherst.

REFERENCES

1. T. Gullion and J. Schaefer, Detection of weak heteronuclear dipolar coupling by rotational-echo double-resonance nuclear magnetic resonance, *Adv. Magn. Reson.* **13,** 57–83 (1989).
2. M. Hong, J. D. Gross, and R. G. Griffin, Site-resolved determination of peptide torsion angle ϕ from the relative orientations of backbone N–H and C–H bonds by solid-state NMR, *J. Phys. Chem. B* **101,** 5869–5874 (1997).
3. M. Hong, Determination of multiple phi-torsion angles in proteins by selective and extensive ^{13}C labeling and two-dimensional solid-state NMR, *J. Magn. Reson.* **139,** 389–401 (1999).
4. K. Saalwächter, R. Graf, and H. W. Spiess, Recoupled polarization transfer heteronuclear multiple-quantum correlation in solids under ultra-fast MAS, *J. Magn. Reson.* **140,** 471–476 (1999).
5. A. Fechtenkötter, K. Saalwächter, M. A. Harbison, K. Müllen, and H. W. Spiess, Highly ordered columnar structures from hexa-*peri*-hexabenzocoronenes—Synthesis, X-ray diffraction, and solid-state heteronuclear multiple-quantum NMR investigations, *Angew. Chem. Int. Ed.* **38,** 3039–3042 (1999).
6. D. Sandström, M. Hong, and K. Schmidt-Rohr, Indentification and mobility of deuterated residues in peptides and proteins by ^{2}H–^{13}C solid-state NMR, *Chem. Phys. Lett.* **300,** 213–220 (1999).

7. I. Sack, A. Goldbourt, S. Vega, and G. Buntkowsky, Deuterium REDOR: Principles and applications for distance measurements, *J. Magn. Reson.* **138,** 54–65 (1999).
8. T. Guillion, Measurement of dipolar interactions between spin-$\frac{1}{2}$ and quadrupolar nuclei by rotational-echo, adiabatic-passage, double-resonance NMR, *Chem. Phys. Lett.* **246,** 325–330 (1995).
9. J. R. Sachleben, V. Frydman, and L. Frydman, Dipolar determinations in solids by relaxation-assisted NMR recoupling, *J. Am. Chem. Soc.* **118,** 9786–9787 (1996).
10. E. R. deAzevedo, W.-G. Hu, T. J. Bonagamba, and K. Schmidt-Rohr, Centerband-only detection of exchange: Efficient analysis of dynamics in solids by NMR, *J. Am. Chem. Soc.* **121,** 8411–8412 (1999).
11. E. R. deAzevedo, W.-G. Hu, T. J. Bonagamba, and K. Schmidt-Rohr, Principles of centerband-only detection of exchange in solid-state NMR, and extensions to 4-time CODEX, *J. Chem. Phys.* **112,** 8988–9001 (2000).
12. H. W. Spiess, Rotation of molecules and nuclear spin relaxation, *in* "NMR Basic Principles and Progress," pp. 55–214, Springer-Verlag, Berlin (1978).
13. J. M. Goetz and J. Schaefer, REDOR dephasing by multiple spins in the presence of molecular motion, *J. Magn. Reson.* **127,** 147–154 (1997).
14. O. W. Sørensen, G. W. Eich, M. H. Levitt, G. Bodenhausen, and R. R. Ernst, Product operator formalism for the description of NMR pulse experiments, *Progr. NMR Spectrosc.* **16,** 163–192 (1983).
15. D. A. Torchia and A. Szabo, Spin–lattice relaxation in solids, *J. Magn. Reson.* **49,** 107–121 (1982).
16. A. Abragam, "The Principles of Nuclear Magnetism," Oxford Univ. Press, Oxford (1961).
17. R. R. Ernst, G. Bodenhausen, and A. Wokaun, "Principles of Nuclear Magnetic Resonance in One and Two Dimensions," Oxford Univ. Press, New York (1987).
18. C. Schmidt, K. J. Kuhn, and H. W. Spiess, Distribution of correlation times in glassy polymers from pulsed deuteron NMR. *Progr. Colloid Polym. Sci.* **71,** 71–76 (1985).
19. K. Schmidt-Rohr and H. W. Spiess, "Multidimensional Solid-State NMR and Polymers," Academic Press, San Diego (1994).
20. T. Terao, H. Miura, and A. Saika, Dipolar SASS NMR spectroscopy: Separation of heteronuclear dipolar powder patterns in rotating solids, *J. Chem. Phys.* **85,** 3816–3826 (1986).
21. A. Naito, P. B. Barker, and C. A. McDowell, Two-dimensional nuclear magnetic resonance studies on a single crystal of L-alanine. Separation of the local dipolar fields; and 2D exchange spectroscopy of the ^{14}N relaxation processes. *J. Chem. Phys.* **81,** 1583–1591 (1984).
22. The given errors are based on a χ^2-analysis which assumed also ratios of T_1^{DQ}/T_1^{SQ} different from ∞.
23. M. S. Lehmann, T. F. Koetzle, and W. C. Hamilton, Precision neutron diffraction structure determination of protein and nucleic acid compounds. I. The crystal and molecular structure of the amino acid L-alanine, *J. Am. Chem. Soc.* **94,** 2657–2660 (1972).
24. R. Destro, R. E. Marsh, and R. Bianchi, A low-temperature (23K) study of L-alanine, *J. Phys. Chem.* **92,** 966–973 (1988).
25. E. R. Henry and A. Szabo, Influence of vibrational motion on solid state line shapes and NMR relaxation, *J. Chem. Phys.* **82,** 4753–4760 (1985).
26. J. L. Derissen, Crystal structure and conformation of methylmalonic acid, *Acta Crystallogr. Sect. B* **26,** 901 (1970).
27. T. Gullion, D. B. Baker, and M. S. Conradi, New, compensated Carr–Purcell sequences, *J. Magn. Reson.* **89,** 479–484, 1990.